Int. J. Bio-Inorg. Hybr. Nanomater., 7(3): 213-219, Autumn 2018

Quantum current modelling on tri-layer graphene nanoribbons in limit degenerate and non-degenerate

Sayed N. Hedayat[1,], M. T. Ahmadi[2], Razali Bin Ismail[3]*

[1,2] *Department of Physics, Faculty of Science, Urmia University, 75175, Urmia, Iran*
[3] *Electronics and Computer Engineering Department, Faculty of Electrical Engineering, University Technology Malaysia, 81310, Malaysia*

Received: 11 April 2017; Accepted: 14 June 2018

ABSTRACT: Graphene is determined by a wonderful carrier transport property and high sensitivity at the surface of a single molecule, making them great as resources used in Nano electronic use. TGN is modeled in form of three honeycomb lattices with pairs of in-equivalent sites as {A1, B1}, {A2, B2}, and {A3, B3} which are located in the top, center and bottom layers, respectively. Trilayer graphene has two types of stable configurations, ABA and ABC stacking orders. In both types, the first two layers are Bernal-stacked, where one sub lattice of the middle layer is located above the center of the hexagons of the bottom layer. The TGN is shown to have different electronic properties which are strongly dependent on the interlayer stacking sequence. ABA-stacked TGN with width and thickness less than De-Broglie wave length can be assumed as a one dimensional material. The present research models transmission coefficient of the Schotcky structure in the graphene-based transistor based on semiconducting channel width and then analysis its quantum properties given dependence on structural parameter. At the same time, the quantum current is presented based on the transmission coefficient for the trilayer graphene. Then, we obtain the quantum current of the proposed structure in the degenerate and non-degenerate states and compare it with experimental data.

Keywords: *Current-Voltage characteristic; Degenerate and nondegenerate regime; Quantum current; Transmission coefficient; Trilayer graphene; Transistor.*

INTRODUCTION

For long time graphene was an "elusive" 2D form of carbon. Ironically it was one of the best theoretically studied carbon allotrope. Graphene model is a starting point for study of all carbon-based systems: graphite, fullerenes, and carbon nanotubes. We will be talking about the tight-binding model in a sense where three electrons of carbon atom, which take part in σ-bonds, are tightly bonded to the atom, while the forth electron creates rather weak π-bonds with its neighbors, giving rise to two π-energy bands called bonding and anti-bonding π-bands in the Brillouin zone (Wallace, 1947). Research on the use of graphene has increased sharply. Physics of graphene is now one of the most active re-

(*) Corresponding Author - e-mail: Sn.hedayat@yahoo.com

search fields. The construction of a new high-speed graphene transistor (Liao, *et al.*, 2010) recognizes the hypothesis that graphene can be the best another to replacing silicon nanotechnology-based devices. After the discovery of graphene in 2004, (Ragheb, *et al.*, 2008), various aspects of the electronic properties of single and three layer graphene research to find the differences between them brought. Multilayers of graphene can be piled up independently relying on the horizontal shift between consecutive graphene planes, which results in a variety of electronic properties and band structures (Avetisyan, *et al.*, 2010). Experiments conducted lately about the multilayer could be relevant in the creation of new electronic devices (Ahmadi, *et al.*, 2009). There are two forms of bulk graphite called ABA- (AB, hexagonal, or Bernal) and ABC- (rhombohedral) stacked TGN with different stacking manners. In TGN with ABA Stacking, the electric field produces band overlap following a proper linear screening which is explained by Thomas-Fermi approximation, whereas in ABC-stacked TGN, it opens an energy gap in the surface-state band at low energy, which results in a strong non-linear to the field amplitude based screening effect. There is spatial inversion symmetry in the lattice of multilayer with even numbered layers similar to that of monolayer graphene. This situation results in a valley degeneracy, in which time-reversal symmetry is not involved (Koshino, *et al.*, 2010). The TGN exhibits a variety of electronic properties that are strongly reliant on the interlayer stacking sequence (Yuan, *et al.*, 2010). TGN as a one dimensional device is in our focus therefore quantum confinement effect will be assumed in two directions; in the other words one Cartesian direction is greater than De-Broglie wavelength. It is also notable that the electrical property of TGN is a strong function of interlayer stacking.

Structure of TGNRs

Unlike single and bilayer graphene, trilayer graphene has two types of stable configurations, ABA (bernal) and ABC (rhombohedral) stacking orders. In both types, the first two layers are Bernal-stacked, where one sub lattice of the middle layer is located above the center of the hexagons of the bottom layer. In ABA-stacked TLG, third layer is exactly on top of the low-

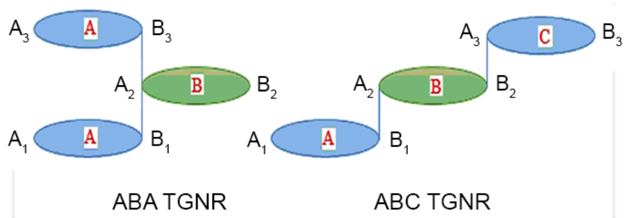

Fig. 1. Structures of TGN with (a) ABA (Bernal) stacking and (b) ABC (rhombohedral) stacking.

est layer. In ABC-stacked trilayer, however, the top layer is shifted by the distance of an atom, so that the top and the bottom layers are also Bernal-stacked. The TGN is shown to have different electronic properties which are strongly dependent on the interlayer stacking sequence. As shown in Fig. 1. ABA-stacked TGN with width and thickness less than De-Broglie wave length (λ_D =10 nm) can be assumed as a one dimensional material. TGN with ABA stacking is modeled in form of three honeycomb lattices with pairs of inequivalent sites as $\{A_1, B_1\}$, $\{A_2, B_2\}$, and $\{A_3, B_3\}$ which are located in the top, center and bottom layers, respectively.

ABC-stacked TGN and its lattice have three layers as a coupled form, in which every coupled form has carbon atoms settling on a honeycomb lattice. A1- B1 pairs are located in the top, while A_2- B_2 pairs are in the heart of layers, and finally A_3- B_3 pairs are placed at the bottom of layers (Koshino, *et al.*, 2009). The ABA-stacked TGN is thermodynamically stable and common. For ABA-stacked TGN, the effective mass model describing the electronic property was developed for the bulk system, and also for few-layer systems. The TGN with ABC stacking has a quite different electronic structure from ABA's. The low-energy band of ABC-stacked TGN is given by the surface states localized at outer-most layers, and an energy gap in its band is opened by the interlayer potential asymmetry, while in ABA-stacked TGN, potential asymmetry causes a band overlapping (Koshino, 2010).

MATERIAL AND METHODS

One of the important concepts in quantum fields is the effect of tunneling that is used in many physical events. Tunneling of particles between prohibited areas can be considered as one of the quantum mechanical re-

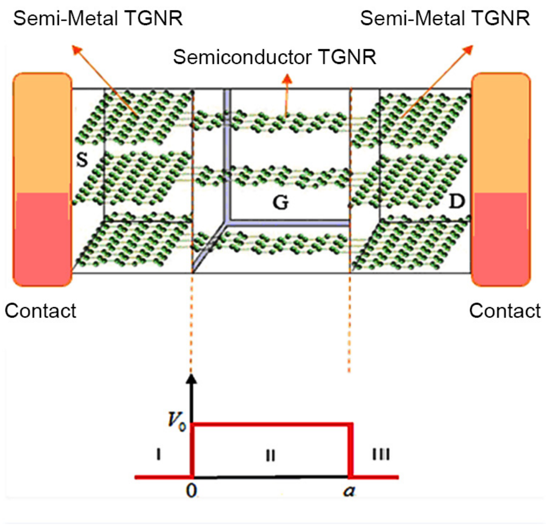

Fig. 2. Channel region barrier in TGNR MOSFET

sults. The numerical calculation of the transmission coefficient was done by Chandra and Christo Moiled. They began to study all parameters in the transmission coefficient and examined the possibility of resonant tunneling in the semiconductor structure. The relationship between wave vectors plays a major role in calculating the transmission coefficient and the density of states. Obtain the transmission coefficient is an important and necessary step for the density of states and quantum current of various electronic devices. As shown in the Fig. 2. The proposed structure includes a semiconductor channel that connected to graphene metals. The quantum transmission coefficient implies number of electrons, overcoming to the junction barriers in the channel. Therefore, the proposed structure consists of three areas.

So, the wave function on the first region is assumed as:

$$\frac{-\hbar^2}{2m}\frac{d^2}{dx^2}\psi_1 = E\psi_1 \rightarrow \psi_1 = A_1 e^{ik_1x} + B_1 e^{-ik_1x} \qquad (1)$$

As for the second region the wave form is as;

$$\left(\frac{-\hbar^2}{2m}\frac{d^2}{dx^2} - V(x)\right)\psi_2 = E\psi_2 \rightarrow \psi_2 = A_2 e^{ik_2x} + B_2 e^{-ik_2x} \qquad (2)$$

On the other hand, the wave form in the last region can be written as:

$$\frac{-\hbar^2}{2m}\frac{d^2}{dx^2}\psi_3 = E\psi_3 \rightarrow \psi_3 = A_3 e^{ik_3x} + B_3 e^{-ik_3x} \qquad (3)$$

The boundary condition need to be satisfied so that to get the A_1, B_1, A_2, B_2 and A_3 parameters we applied in continuity conditions. So by using the proposed boundary condition the coefficient A_3 can be written as:

$$A_3 = 4k_1k_2A_1e^{-ik_1a}\left[4k_1k_2\cos(k_2a) - 2i\left(k_1^2 + k_2^2\right)\sin(k_2a)\right]^{-1} \qquad (4)$$

Transmission coefficient in TGNRs

The transmission coefficient is applied in physics and Nano electronic application once wave propagation in a medium containing discontinuities is considered and hence it assumed as;

$$T = \left|\frac{A_3}{A_1}\right|^2 \qquad (5)$$

This equation is rewritten upon presence of transmission coefficient furthermore, in state $E<V_0$ for TGNR as below:

$$T = \frac{1}{1+\left(\frac{k_1^2 + k_2^2}{2k_1k_2}\right)^2 \mathrm{Sinh}^2(k_2L)} \qquad (6)$$

Where

$$k_1^2 = k_3^2 = \left(\frac{A + (x + \sqrt{3}\sqrt{B + x^2/3})^{\frac{2}{3}}}{(x + \sqrt{3}\sqrt{B + x^2/3})^{\frac{1}{3}} C}\right)^2$$

and

$$k_2^2 = \left(\frac{A + ((x+d) + \sqrt{3}\sqrt{B + (x+d)^2/3})^{\frac{2}{3}}}{((x+d) + \sqrt{3}\sqrt{B + (x+d)^2/3})^{\frac{1}{3}} C}\right)^2$$

represents quantum wave vectors in the source and drain terminals respectively as it was shown Fig. 2. As it is shown in Fig. 3, length effect on transmission coefficient is analyzed.

We define

$$-9(E - E_{1g})\beta^2 = x, -9(E_{1g} - E_{2g})\beta^2 = d,$$

$$(2)^{\frac{2}{3}}(3)^{\frac{1}{3}}\alpha\beta = A, -4\alpha^3\beta^3 = B, 2^{\frac{1}{3}}3^{\frac{2}{3}}\beta = C$$

Therefore, the transmission coefficient for the tri-layer graphene nanoribbons is defined as follows;

$$T=\frac{4\left(\frac{A+(x+\sqrt{3}\sqrt{B+\frac{x^2}{3}})^{\frac{2}{3}}}{(x+\sqrt{3}\sqrt{B+\frac{x^2}{3}})^{\frac{1}{3}}C}\right)^2\left(\frac{A+((x+d)+\sqrt{3}\sqrt{B+\frac{(x+d)^2}{3}})^{\frac{2}{3}}}{((x+d)+\sqrt{3}\sqrt{B+\frac{(x+d)^2}{3}})^{\frac{1}{3}}C}\right)^2}{4\left(\frac{A+(x+\sqrt{3}\sqrt{B+\frac{x^2}{3}})^{\frac{2}{3}}}{(x+\sqrt{3}\sqrt{B+\frac{x^2}{3}})^{\frac{1}{3}}C}\right)^2\left(\frac{A+((x+d)+\sqrt{3}\sqrt{B+\frac{(x+d)^2}{3}})^{\frac{2}{3}}}{((x+d)+\sqrt{3}\sqrt{B+\frac{(x+d)^2}{3}})^{\frac{1}{3}}C}\right)^2+\left(\left(\frac{A+(x+\sqrt{3}\sqrt{B+\frac{x^2}{3}})^{\frac{2}{3}}}{(x+\sqrt{3}\sqrt{B+\frac{x^2}{3}})^{\frac{1}{3}}C}\right)^2+\left(\frac{A+((x+d)+\sqrt{3}\sqrt{B+\frac{(x+d)^2}{3}})^{\frac{2}{3}}}{((x+d)+\sqrt{3}\sqrt{B+\frac{(x+d)^2}{3}})^{\frac{1}{3}}C}\right)^2\right)^2\sinh^2\left(\left(\frac{A+((x+d)+\sqrt{3}\sqrt{B+\frac{(x+d)^2}{3}})^{\frac{2}{3}}}{((x+d)+\sqrt{3}\sqrt{B+\frac{(x+d)^2}{3}})^{\frac{1}{3}}C}\right)a\right)} \tag{7}$$

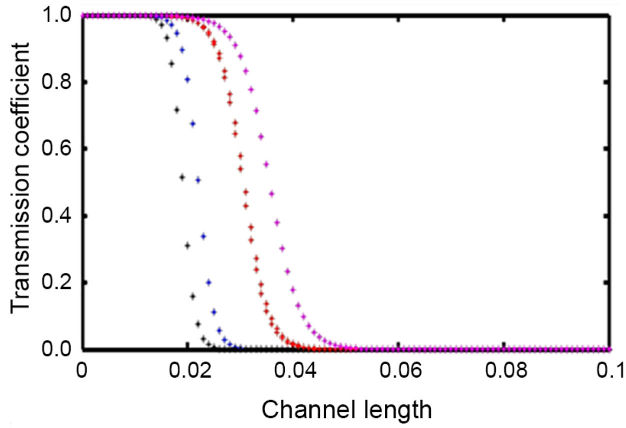

Fig. 3. Illustration of transmission coefficient of trilayer graphene nanoribbon versus channel length (x= -10 (Violet), x=1 (Red), x=50 (blue) and x=100 (black)).

As depicted in Fig. 3, the transmission coefficient of proposed model is plotted versus the channel length and minimum transmission coefficient is close to end of channel. Also x dependent on energy, and due to the quantum effects, with by increasing x the length of the channel is smaller.

RESULT AND DISCUSSION

Quantum current in TGNRs

It is obvious that, the transmission coefficient for higher values of channel length is lowered. The quantum current based Landauer formalism have been reported in as

$$I=\int_{E-\frac{E_g}{2}}^{E+\frac{E_g}{2}} T(E)f(E)dE \tag{8}$$

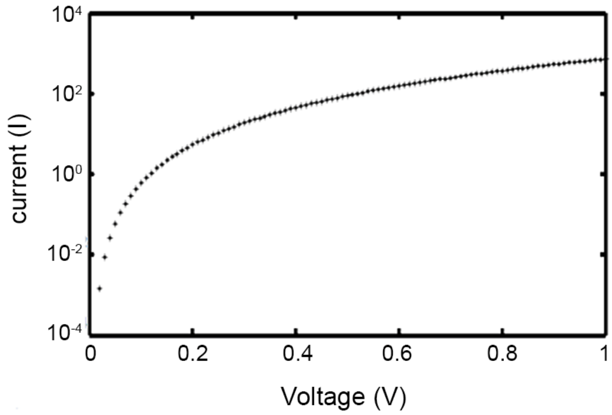

Fig. 4. A plot on I-V model of TGNR

Where denoted on Fermi Dirac distribution function which implies to probability of occupied levels at energy E. Given wave vector and transmission coefficient in the simplified model quantum current is modified as:

This equation might be numerically solved for different potential. Thus, the proposed quantum current model of trilayer graphene nanoribbon under nanostructured regime by the Current-Voltage characteristic is evaluated in Fig. 4. If the voltage in each region is changed, on the other hand, the geometrical parameter effect on the transport factor is investigated as shown in Fig. 5.

Degenerate and non-degenerate regimes in TGNRs

As number of carriers increases, device will operate in degenerate limit. Degenerate regime plays an important role on quantum current research in the Nanoscale devices. In the degenerate regime, $E-E_F<3k_BT$, also, degeneracy of TGNR can be defined once Fermi

$$I=\int_0^{\eta}\frac{4\left(\frac{A+(x+\sqrt{3}\sqrt{B+\frac{x^2}{3}})^{\frac{2}{3}}}{(x+\sqrt{3}\sqrt{B+\frac{x^2}{3}})^{\frac{1}{3}}C}\right)^2\left(\frac{A+((x+d)+\sqrt{3}\sqrt{B+\frac{(x+d)^2}{3}})^{\frac{2}{3}}}{((x+d)+\sqrt{3}\sqrt{B+\frac{(x+d)^2}{3}})^{\frac{1}{3}}C}\right)^2 k_BT}{4\left(\frac{A+(x+\sqrt{3}\sqrt{B+\frac{x^2}{3}})^{\frac{2}{3}}}{(x+\sqrt{3}\sqrt{B+\frac{x^2}{3}})^{\frac{1}{3}}C}\right)^2\left(\frac{A+((x+d)+\sqrt{3}\sqrt{B+\frac{(x+d)^2}{3}})^{\frac{2}{3}}}{((x+d)+\sqrt{3}\sqrt{B+\frac{(x+d)^2}{3}})^{\frac{1}{3}}C}\right)^2+\left(\left(\frac{A+(x+\sqrt{3}\sqrt{B+\frac{x^2}{3}})^{\frac{2}{3}}}{(x+\sqrt{3}\sqrt{B+\frac{x^2}{3}})^{\frac{1}{3}}C}\right)^2+\left(\frac{A+((x+d)+\sqrt{3}\sqrt{B+\frac{(x+d)^2}{3}})^{\frac{2}{3}}}{((x+d)+\sqrt{3}\sqrt{B+\frac{(x+d)^2}{3}})^{\frac{1}{3}}C}\right)^2\right)^2\sinh^2\left(\left(\frac{A+((x+d)+\sqrt{3}\sqrt{B+\frac{(x+d)^2}{3}})^{\frac{2}{3}}}{((x+d)+\sqrt{3}\sqrt{B+\frac{(x+d)^2}{3}})^{\frac{1}{3}}C}\right)a\right)}*\frac{1}{\exp(x-\eta)}dx \tag{9}$$

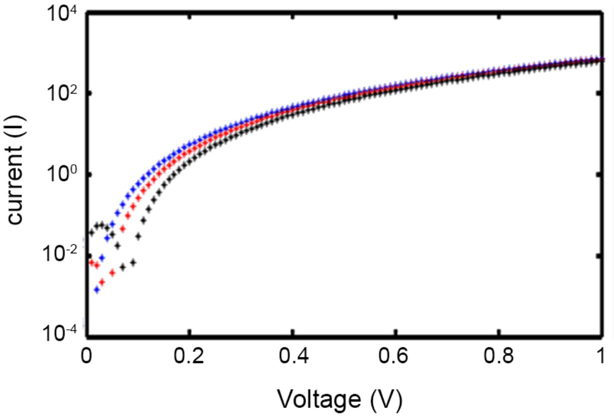

Fig. 5. The quantum current variation in TGNR based transistor (black line indicates voltage 0.03 volt, red line for voltage 0.06 volt, blue line for voltage 0.08 volt).

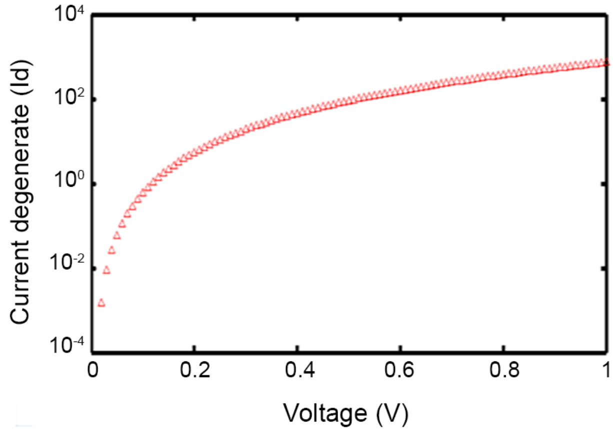

Fig. 6. I-V model of TGNR in degenerate approximation

probability function equals one f(E)=1. For the non-degenerate regime in the contrary, $E-E_F<3k_BT$ then we can write $f(E)=\exp(E_f-E/k_BT)$. In the other words, given very small amount of x-η in this regime, expr(x-η) can be neglected. So quantum current in degenerate approximation is (Hedayat, *et al.*, 2017);

As it can be seen in the Fig. 6, quantum current in the range larger than zero leads to the degenerate approximation on TGNR.

the quantum current in non-degenerate regime can be modified by exponential function so that:

Finally, Fig. 8. illustrates comparison of quantum current, model and non-degenerate regime quantum current.

As shown in the Fig. 8, voltage in the range of more than 0.5 volt leads to the degenerate approximation on TGNR. Non-degenerate approximation have been

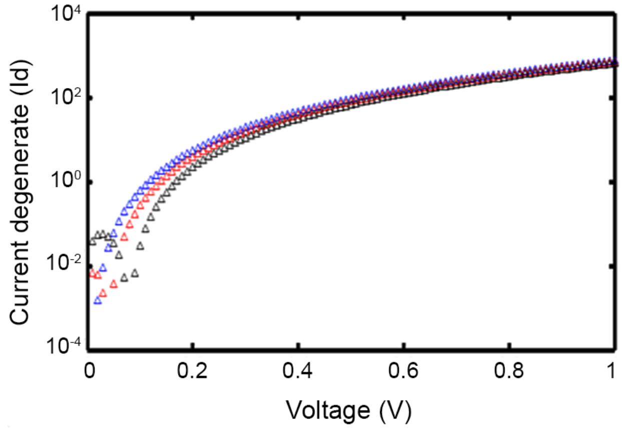

Fig. 7. The quantum current in degenerate regime variation in TGNR based transistor (black line indicates voltage 0.03 volt, red line for voltage 0.06 volt, blue line for voltage 0.08 volt).

made known among the reserve more than $3K_BT$ preliminary also the conduction or valance band edging

$$I_d=\int_0^{\eta}\frac{4\left(\frac{A+(x+\sqrt{3}\sqrt{B+x^2/3})^{\frac{2}{3}}}{(x+\sqrt{3}\sqrt{B+x^2/3})^{\frac{1}{3}}C}\right)^2\left(\frac{A+((x+d)+\sqrt{3}\sqrt{B+(x+d)^2/3})^{\frac{2}{3}}}{((x+d)+\sqrt{3}\sqrt{B+(x+d)^2/3})^{\frac{1}{3}}C}\right)^2 k_BT}{4\left(\frac{A+(x+\sqrt{3}\sqrt{B+x^2/3})^{\frac{2}{3}}}{(x+\sqrt{3}\sqrt{B+x^2/3})^{\frac{1}{3}}C}\right)^2\left(\frac{A+((x+d)+\sqrt{3}\sqrt{B+(x+d)^2/3})^{\frac{2}{3}}}{((x+d)+\sqrt{3}\sqrt{B+(x+d)^2/3})^{\frac{1}{3}}C}\right)^2+\left(\left(\frac{A+(x+\sqrt{3}\sqrt{B+x^2/3})^{\frac{2}{3}}}{(x+\sqrt{3}\sqrt{B+x^2/3})^{\frac{1}{3}}C}\right)^2+\left(\frac{A+((x+d)+\sqrt{3}\sqrt{B+(x+d)^2/3})^{\frac{2}{3}}}{((x+d)+\sqrt{3}\sqrt{B+(x+d)^2/3})^{\frac{1}{3}}C}\right)^2\right)^2\sinh^2\left(\left(\frac{A+((x+d)+\sqrt{3}\sqrt{B+(x+d)^2/3})^{\frac{2}{3}}}{((x+d)+\sqrt{3}\sqrt{B+(x+d)^2/3})^{\frac{1}{3}}C}\right)a\right)}dx \tag{10}$$

$$I_{nd}=\int_0^{\eta}\frac{4\left(\frac{A+(x+\sqrt{3}\sqrt{B+x^2/3})^{\frac{2}{3}}}{(x+\sqrt{3}\sqrt{B+x^2/3})^{\frac{1}{3}}C}\right)^2\left(\frac{A+((x+d)+\sqrt{3}\sqrt{B+(x+d)^2/3})^{\frac{2}{3}}}{((x+d)+\sqrt{3}\sqrt{B+(x+d)^2/3})^{\frac{1}{3}}C}\right)^2 e^{\eta}k_BT}{4\left(\frac{A+(x+\sqrt{3}\sqrt{B+x^2/3})^{\frac{2}{3}}}{(x+\sqrt{3}\sqrt{B+x^2/3})^{\frac{1}{3}}C}\right)^2\left(\frac{A+((x+d)+\sqrt{3}\sqrt{B+(x+d)^2/3})^{\frac{2}{3}}}{((x+d)+\sqrt{3}\sqrt{B+(x+d)^2/3})^{\frac{1}{3}}C}\right)^2+\left(\left(\frac{A+(x+\sqrt{3}\sqrt{B+x^2/3})^{\frac{2}{3}}}{(x+\sqrt{3}\sqrt{B+x^2/3})^{\frac{1}{3}}C}\right)^2+\left(\frac{A+((x+d)+\sqrt{3}\sqrt{B+(x+d)^2/3})^{\frac{2}{3}}}{((x+d)+\sqrt{3}\sqrt{B+(x+d)^2/3})^{\frac{1}{3}}C}\right)^2\right)^2\sinh^2\left(\left(\frac{A+((x+d)+\sqrt{3}\sqrt{B+(x+d)^2/3})^{\frac{2}{3}}}{((x+d)+\sqrt{3}\sqrt{B+(x+d)^2/3})^{\frac{1}{3}}C}\right)a\right)} \tag{11}$$

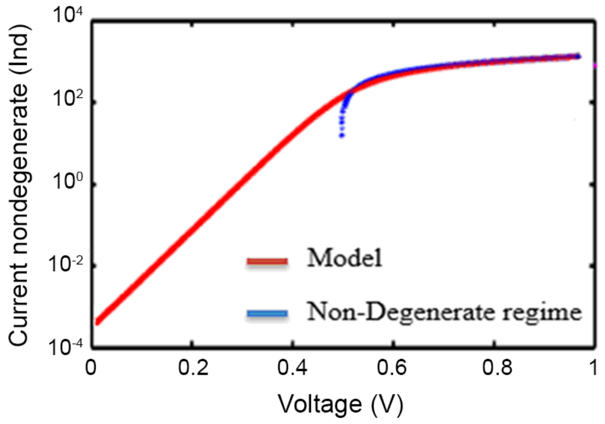

Fig. 8. Comparison of the quantum current and non-degenerate regime quantum current

in the form of band gap in the neighborhood of the Fermi plane. As per the proposed model, quantum current is simulated as a basic characteristic of a transistor and as for conventional methods, the same trend is investigated.

CONCLUSIONS

Graphene is fraught with unique carrier transport property and high sensitivity upon single molecule level, which introduced it as promising material in biosensor application. This study focused on trilayer graphene nanoribbons and analytical model of quantum current presented. In this paper quantum current as a basic parameter in both degenerate and non-degenerate regimes was explored too, and compare it with experimental data that, there is good agreement between the proposed model and the experimental data. Also trilayer Graphene nanoribbons transistors that, work based on quantum current, the current-voltage diagram is very close to degeneracy.

ACKNOELDGMENT

Authors would like to acknowledge the financial support from Research University grant of the Urmia University. Also thanks to the Re¬search Management Center of Urmia University for providing excel¬lent research environment in which to complete this work.

REFERENCES

Wallace, P. R., (1947). The band theory of graphite. Phys. Rev., 71 (9): 622-634.

Liao, L., (2010). High-speed graphene transistors with a self-aligned nanowire gate. Nature, 467: 305-308.

Ragheb, T. and Massoud, Y., (2008). On the modeling of resistance in graphene nanoribbon (GNR) for future interconnect applications. in Computer-Aided Design, 2008. ICCAD 2008. IEEE/ACM International Conference on. 2008.

Avetisyan, A. A., (2010). Stacking Order dependent Electric Field tuning of the Band Gap in Graphene Multilayers. Phys. Rev. B, 81: 115432-10.

Ahmadi, M. T., (2009). MOSFET-Like Carbon Nanotube Field Effect Transistor Model, Nanotech Conference & Expo 2009, Technical Proceedings, 3: 574-579.

Koshino, M. and McCann, E., (2010). Parity and valley degeneracy in multilayer graphene. Phys. Rev. B, 81 (11): 115315.

Yuan, S., Raedt, H. De, and Katsnelson, M. I., (2010). Electronic Transport in Disordered Bilayer and Trilayer Graphene. Phys. Rev. B, 82: 235409.

Koshino, M. and McCann, E., (2009). Trigonal warping and Berry’s phase Npi in ABC- stacked multilayer graphene. Phys. Rev. B, 80: 165409.

Koshino, M., (2009). Interlayer screening effect in graphene multilayers with ABA and ABC stacking. Phys. Rev. B, 81: 125304.

Sayed N. Hedayat, M. T. Ahmadi, H. Sedghi, H. Goudarzi, and Razali Bin Ismail, (2017). Transmission Coefficient and Quantum Current in Graphene Nanoribbons. Advanced Science, Engineering and Medicine, 9(4): 278-281.

AUTHOR (S) BIOSKETCHES

Seyed Norollah Hedayat, PhD., Department of physics, Faculty of science, Urmia University, 75175, Urmia, Iran, *Email: Sn.hedayat@yahoo.com*

Mohammad Taghi Ahmadi, Professor, Department of physics, Faculty of science, Urmia University, 75175, Urmia, Iran

Razali Bin Ismail, Professor, Electronics and Computer Engineering Department, Faculty of Electrical Engineering, University Technology Malaysia, 81310 Johor Bahro, Malaysia